Current Zoology, 2026, 00, 1–18
https://doi.org/10.1093/cz/zoag023
Published: 30 March 2026
Original article

Skeletal and dental anomalies provide insights into insular vertebrate zoology and evolution in Plio-Holocene Menorca, Western Mediterranean

Blanca Moncunill-Solé [a,b,c*], Josep Quintana Cardona [d,e], Alejandro Blanco [a,b] and Bruce M. Rothschild [f]

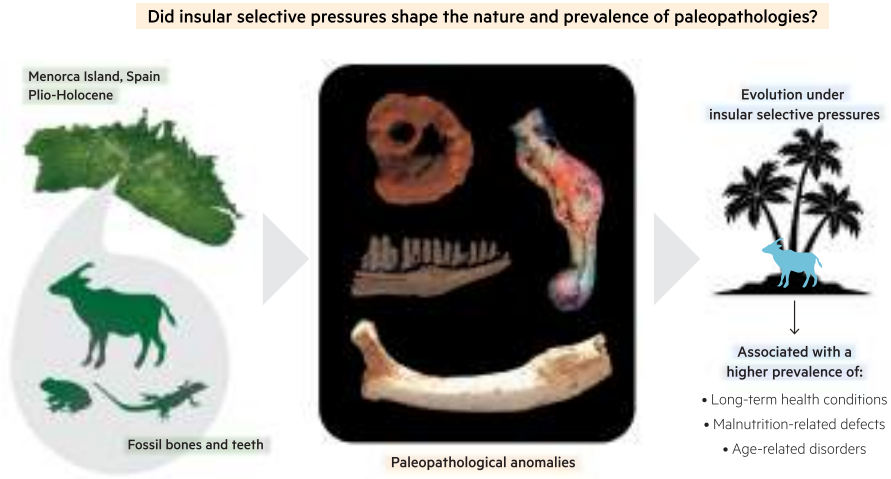
[a]Grupo BIOpast, Departamento de Física e Ciencias da Terra, Universidade da Coruña, Rúa da Fraga 10, A Coruña 15008, Spain
[b]Centro de Innovación Tecnolóxica en Edificación e Enxeñería Civil (CITEEC), Universidade da Coruña, Campus de Elviña s/n, A Coruña 15008, Spain
[c]Centro de Investigação em Biodiversidade e Recursos Genéticos (CIBIO), Universidade do Porto, Rúa Armando Quintas 7, Vairão 4485-661, Portugal
[d]Institut Català de Paleontologia Miquel Crusafont, Campus de la Universitat Autònoma de Barcelona, Carrer de les columnes s/n, Cerdanyola del Vallès 08193, Spain
[e]c/Gustau Mas 79 1r, Ciutadella de Menorca 07760, Spain
[f]Indiana University Healthy, 2401W University Ave, Muncie, IN 47303, USA
*Address correspondence to Blanca Moncunill-Solé. E-mail: blanca.moncunill@udc.es.
Handling editor: Diego Astúa

Abstract

The examination of paleopathological abnormalities provides valuable insights into the biology of past species. Considering the particular selective pressures of islands, their faunas may exhibit anomalies distinct in type or prevalence compared with mainland relatives. Here, we report and describe 10 fossil remains showing pathological conditions from 3 insular vertebrates: *Latonia* sp. (Lissamphibia), *Podarcis lilfordi* (Lepidosauria), and *Myotragus balearicus* (Mammalia) (Pliocene-Quaternary; Menorca, Balearic Islands, Spain). Macroscopic- and microscopic techniques were employed to diagnose the disease, determine etiology, and assess the cause of death. Our findings reveal (1) predominantly healed fractures in *Latonia*; (2) infections complicated by fibresceses (fibrous abscesses) in *P. lilfordi*; and (3) neoplasms and probable congenital malformations in *M. balearicus*. These results represent the first paleopathological descriptions for *Latonia* and *P. lilfordi* and the first identification of neoplasms in *Myotragus*. Certain diagnosed abnormalities are unique and rare and have not been previously reported in either extinct or extant relatives. A review of pathological cases in insular taxa has revealed a higher prevalence of long-term health conditions, malnutrition-related defects, and age-related disorders. By expanding biological knowledge of these species, our results also contribute to a broader understanding of vertebrate ecology under insular regimes through empirical observations in interdisciplinary research.

Keywords imaging techniques, insular environments, insular syndrome, paleopathology, paleozoology

Graphical abstract



Received: October 2, 2025. **Accepted:** March 24, 2026
© The Author(s) 2026. Published by Oxford University Press on behalf of Editorial Office, Current Zoology.
This is an Open Access article distributed under the terms of the Creative Commons Attribution License (https://creativecommons.org/licenses/by/4.0/), which permits unrestricted reuse, distribution, and reproduction in any medium, provided the original work is properly cited.

Downloaded from academic.oup.com/cz/advance-article/doi/10.1093/cz/zoag023/8556684 by guest on 23 October 2026

Paleopathological conditions refer to abnormalities recognized in the remains of fossil organisms. Their research allows gaining valuable insights into the biology, behavior, and ecology of past taxa, as well as in the origin, distribution, and evolution of diseases over time (Rothschild and Martin 2006; Waldron 2009, 2012; Rothschild and Laub 2013; Moncunill-Solé et al. 2019, 2024; Grauer 2022; Rothschild et al. 2023). The first paleopathological observations and publications date back to the 18th century (Esper 1774), although it was not until the mid-20th century that the earliest compendia, which are still widely used today, were published (Brothwell and Sandison 1967; Baker and Brothwell 1980; Grauer 2012; Rothschild et al. 2023; among others). The final objective of the paleopathological research has changed significantly over these 3 centuries. In addition to providing descriptions and differential diagnoses (the basis of paleopathological analysis), current paleopathologists go a step further, revealing the etiology of diseases, elaborating quantitative reports, and enlightening the environmental or evolutionary drivers of several diseases. In modern paleontological paleopathology (see below), researchers aim to uncover the frequency and types of injuries in fossil populations, species, or larger taxonomic groups (Witzmann and Asbach 2022). The most recent approaches tend to be multidisciplinary, multifocal, and based on complete populations rather than isolated cases. Taking advantage of the technological boom, the leading-edge non-invasive techniques of the moment are used (e.g., X-ray-computed tomography, synchrotron scanning, electron microscopes, immunofluorescence, or mass spectrometers), providing more rigorous examinations and most likely differential diagnoses without the destruction of valuable and singular fossil remains (Grauer 2012; Rothschild et al. 2023).

Paleontological paleopathology provides a deep-time perspective and is focused on the evolutionary history of illness in organisms up to 500 million years old (Witzmann et al. 2021; Rothschild et al. 2023). At present, thousands of cases of diseases in fossil non-human vertebrates have been reported and published. Outstanding among the most common ones are traumatic injuries (e.g., bite wounds or bone fractures), neoplastic disorders, infections (e.g., osteomyelitis or tuberculosis), metabolic diseases, and developmental (or congenital) anomalies (Baker and Brothwell 1980; Witzmann and Asbach 2022; Rothschild et al. 2023; among others). Traumatic injuries are very common in fossils and are used to reconstruct the behavior and lifestyle of past taxa as well as their relationship with concurrent organisms and environment. By contrast, neoplastic diseases show a low prevalence (with only 2 cases identified undisputedly in Paleozoic vertebrate remains: osteoma in an Early Carboniferous ray-finned fish and odontoma in an early Permian gorgonopsian) (Moodie 1927; White 1927; Whitney et al. 2017), though its incidence rate has increased from Paleozoic to historical times. The occurrence of infectious and metabolic diseases in the fossil record is not as high as for other conditions (Witzmann and Asbach 2022). The oldest bony infectious lesions have been reported in Carboniferous organisms, but a scarce number of osteomyelitis cases were diagnosed in Pleistocene taxa (e.g., cave bear). Teratologies are relatively common in the fossil record, affecting mainly teeth and axial skeleton, and, in certain cases, can shed light on environmental or behavior factors [see Witzmann and Asbach (2022) for more details].

Bones and teeth with lesions and injuries have been recovered from several Plio-Holocene fossil localities on the island of Menorca (Balearic Islands, Spain; Western Mediterranean). They belong to endemic species of anurans, lizards, and ruminants (see *Materials and methods* section for descriptions). Ecologically, islands are recognized as biodiversity hotspots with high levels of endemism, though their biotas are generally impoverished, unbalanced, and disharmonic (Whittaker and Fernández-Palacios 2007). Moreover, insular environments are recognized by reduced resources and lower extrinsic mortality rates. In both extant and extinct faunas, specific morphologies, life history traits, and biological and behavioral characteristics have been interpreted as eco-evolutionary responses to these distinctive selective pressures (e.g., Sondaar 1977; Moncunill-Solé 2021; Palombo and Moncunill-Solé 2025). Given that insularity influence species' survival and mortality rates, it is proposed that insular faunas may exhibit distinct paleopathological types and prevalence (e.g., different kinds of abnormalities than mainland species) (Moncunill-Solé et al. 2019, 2024, and references therein). This should be particularly evident in the fossil record, which is free of anthropogenic impact.

In this context, we hypothesize that insular selective pressures have shaped both the nature and prevalence of palaeopathologies in Plio-Holocene Menorcan endemic species, leading to patterns that differ from those observed in continental relatives (e.g., higher incidence of long-term or chronic diseases compared to continental relatives). The objective of the present research is to provide a systematic description of these anomalous bones and teeth, aiming to identify their etiology and, where possible, their role in mortality. By integrating paleopathological and insular ecology data, this study seeks to infer behavioral and life history features that cannot be attained through other approaches. In addition, it will provide a review of the relationship between paleopathological disorders and insularity, contributing to a broader zoological understanding of vertebrate evolution under insular regimes.

Materials and methods

Study specimens and site

We analyze 10 paleopathological specimens belonging to 3 vertebrate taxa: *Latonia* von Meyer, 1843 ($N = 5$) (Lissamphibia, Alytidae), *Podarcis lilfordi* Günther, 1874 ($N = 2$) (Lepidosauria, Lacertidae), and *Myotragus balearicus* Bate, 1909 ($N = 3$) (Mammalia, Bovidae) (Fig. 1). These specimens were retrieved from 4 fossil localities of Menorca (Balearic Islands, Spain; Western Mediterranean): Punta Nati 6 (Pliocene), Punta Esquitxador 17 (Upper Pleistocene), Sa Cigonya (Pleistocene), and Pas d'en Revull (Holocene) (Supplementary Appendix S1 and Supplementary Figure S1 for a detailed geological setting of them). The remains are hosted in the facilities of the Institut Català de Paleontologia Miquel Crusafont (collection acronym IPS; Sabadell, Spain) and Bep Quintana Collection (collection acronym CBQ; Ciutadella de Menorca, Spain). Refer to Table 1 for a complete description of the material.

Downloaded from academic.oup.com/cz/advance-article/doi/10.1093/cz/zoag023/8556684 by guest on 23 October 2026

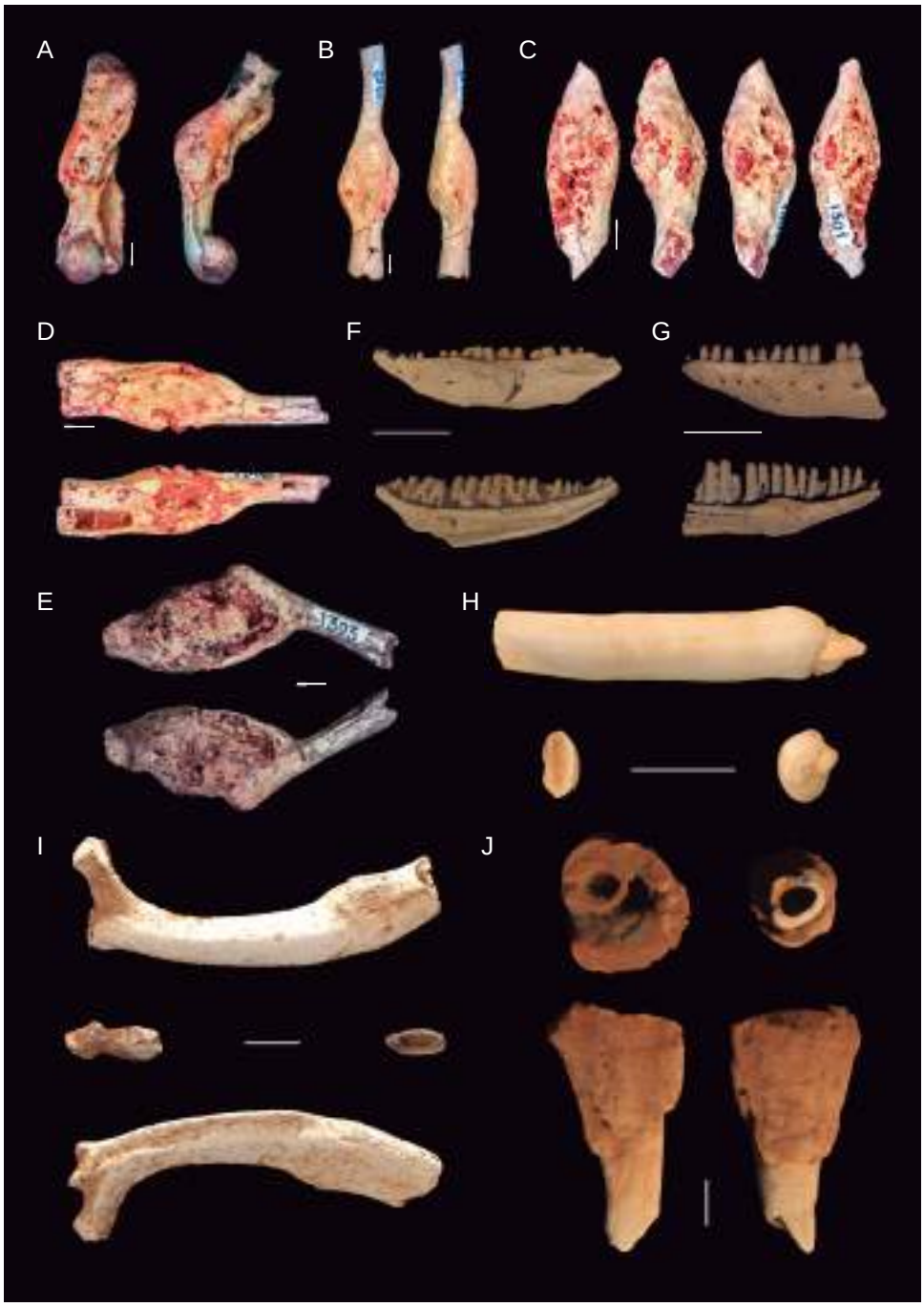


Figure 1 Fossil specimens with abnormal conditions from Plio-Holocene localities in Menorca (Balearic Islands, Spain; Western Mediterranean). *Latonia* sp. a) IPS15200, right humerus. In ventral (left) and lateral (right) views. Proximal end on the top, distal end on the bottom. b) IPS15748, left femur. In ventral (left) and lateral (right) views. Proximal end on the top, distal end on the bottom. c) IPS16079, undetermined diaphysis of a long bone. d) IPS16080, right tibiofibula. In dorsal (top) and ventral (bottom) views. Proximal end on the right, distal end on the left. e) IPS16081, undetermined long bone (?right femur). In ventral (top) and dorsal (bottom) view. Proximal end on the right, distal end on the left; *Podarcis lilfordi*. f) CBQ-368a, left dentary. In labial (top) and lingual (bottom) views. g) CBQ-368b, left dentary. In labial (top) and lingual (bottom) views; *Myotragus balearicus*. h) CBQ-928, lower permanent incisive (i1). In labial (top), occlusal (left bottom), and basal (right bottom) views. i) CBQ-SN, right rib. In lateral (top), proximal (left middle), distal (right middle) and medial (bottom) views. j) CBQ-1888, diaphysis of long bone. In proximo-distal (top images) and antero-posterior (bottom images) views. Refer to Table 1 for the localities and age. Scale equals 3 mm in *Latonia* and *P. lilfordi* specimens, and 1 cm in *M. balearicus* remains.

Examination, imaging, and diagnostic methods

We decided to implement a 2-fold approach to analyze the fossil specimens, including both macroscopic and radiologic imaging procedures. Invasive methods, such as histological, geochemical, genetic, and genomic analyses, were excluded because of their destructive nature and the small size of the study sample.

Gross examination and surface imaging allow for the provision of detailed and consistent descriptions of the lesions. Remains are

Downloaded from academic.oup.com/cz/advance-article/doi/10.1093/cz/zoag023/8556684 by guest on 23 October 2026

Table 1 Paleopathological specimens under study.

ID	Taxon	Bone/tooth element	Locality: site and age	Locality: associated fauna
IPS15200	*Latonia* sp.	Right humerus	Punta Nati 6 (Pliocene)	• *Cheirogaster gymnesica* • *Latonia* sp. • *Nuralagus rex* • Endemic species and genera of birds
IPS15748	*Latonia* sp.	Left femur (diaphysis)		
IPS16079	*Latonia* sp.	Unknown (diaphysis of long bone)		
IPS16080	*Latonia* sp.	Right tibiofibula (distal epiphysis)		
IPS16081	*Latonia* sp.	Unknown, possible right femur		
CBQ-368a	*Podarcis lilfordi*	Left dentary	Punta Esquitxador 17 (Upper Pleistocene)	• *Podarcis lilfordi* • *Hypnomys mahonensis* • Birds, including: *Puffinus* sp. 1 and 2, *Hydrobates pelagicus*, *Coturnix* cf. *coturnix*, *Rallus* cf. *aquaticus*, *Rallus* sp. 2, *Gallinula chloropus*, *Scolopax rusticola*, *Tyto balearica*, *Athene noctua*, *Erithacus* sp., *Sylvia* sp., Passeriformes indet.
CBQ-368b	*Podarcis lilfordi*	Left dentary		
CBQ-928	*Myotragus balearicus*	Lower permanent incisor (i1)	Pas d'en Revull (Holocene)	• Terrestrial mollusks • *Oryctolagus cuniculus* • *Myotragus balearicus* • Undetermined vertebrates (mammals, amphibians, reptiles and birds)
CBQ-1888	*Myotragus balearicus*	Undetermined long bone, possible tibia (proximal epiphysis)	Sa Cigonya (Pleistocene)	• *Podarcis lilfordi* • *Discoglossus* sp. • *Nesiotites* sp. • *Hypnomys* sp. • *Myotragus balearicus* • Birds, including: *Accipiter nisus, Burhinus oedicnemus, Turdus* sp., *Pica* sp. and Corvidae indet.
CBQ-S/N	*Myotragus balearicus*	Right rib (proximal end and fragmented body)		

Columns: Identification number (ID), taxon, bone/tooth element, and locality information (site and age; and associated fauna). See text for references.

examined visually to identify surface skeletal abnormalities (e.g., bone alterations in the articular and cortical surfaces, as well as growth plates at non-epiphyseal sites) and mapping the distribution of occurrences on each bone (Rothschild and Martin 2006; Rothschild et al. 2023). All deviations from normal structure are recorded, noting those of taphonomic origin. In addition, standardized metric measurements and photographs are taken using a Mitutoyo Absolute Digimatic CD-8"AX caliper, a Canon EOS 250D digital camera (zoom lens EF-S18-55 mm f/4-5.6 IS STM), and a DINO-lite Edge (model AM7915MZTL). On the other hand, radiological procedures are performed using non-invasive cross-sectional imaging techniques. The obtained images allow for observation of inner bone structures of interest and the evaluation of possible histological and microstructural changes without causing damage to the fossil remains (Grauer 2022; Rothschild et al. 2023). The 10 specimens under study are scanned using a Bruker Skyscan 1172 X-ray microtomograph housed at the "Estación de Bioloxía Mariña da Graña" facilities (Universidade de Santiago de Compostela USC, Ferrol, Spain) with the following settings: voxel size of 10.07 μm, voltage of 100 kV, and current of 100 μA. The software Dragonfly 2022.2 (version 2022.2.0.1409) [Computer software; Comet Technologies Canada Inc., Montreal, Canada. https://www.theobjects.com/dragonfly] is used for the visualization, processing, and analysis of data. Backups are stored in the virtual collections of the BIOpast group, Physics and Earth Science Department of the Universidade da Coruña (UDC, A Coruña, Spain), and the Institut Català de Paleontologia Miquel Crusafont (ICP, Sabadell, Spain). In addition, the volumetric image series (microCT scans, raw data) of the specimens are hosted on the online 3D scientific data repository MorphoSource (https://www.morphosource.org/projects/000758818), including metadata, and ensuring transparency of the research.

The diagnoses are achieved by comparing the pathological lesions with those of extant homologous species (phylogenetic approach, following the terminology of Witzmann and Asbach 2022). It is accepted that pathogenesis does not change over time and that diseases proceed in the same way in extant and extinct specimens (uniformitarian principle) (Witzmann and Asbach 2022; Rothschild et al. 2023; and references therein). Anomalies resulting from postmortem taphonomic processes are not considered. Following the steps involved in the differential diagnosis process, a range of possible diagnoses is initially considered. Subsequently, those that did not fit with the observed lesions are accurately ruled out. A differential diagnosis is determined considering

Downloaded from academic.oup.com/cz/advance-article/doi/10.1093/cz/zoag023/8556684 by guest on 23 October 2026

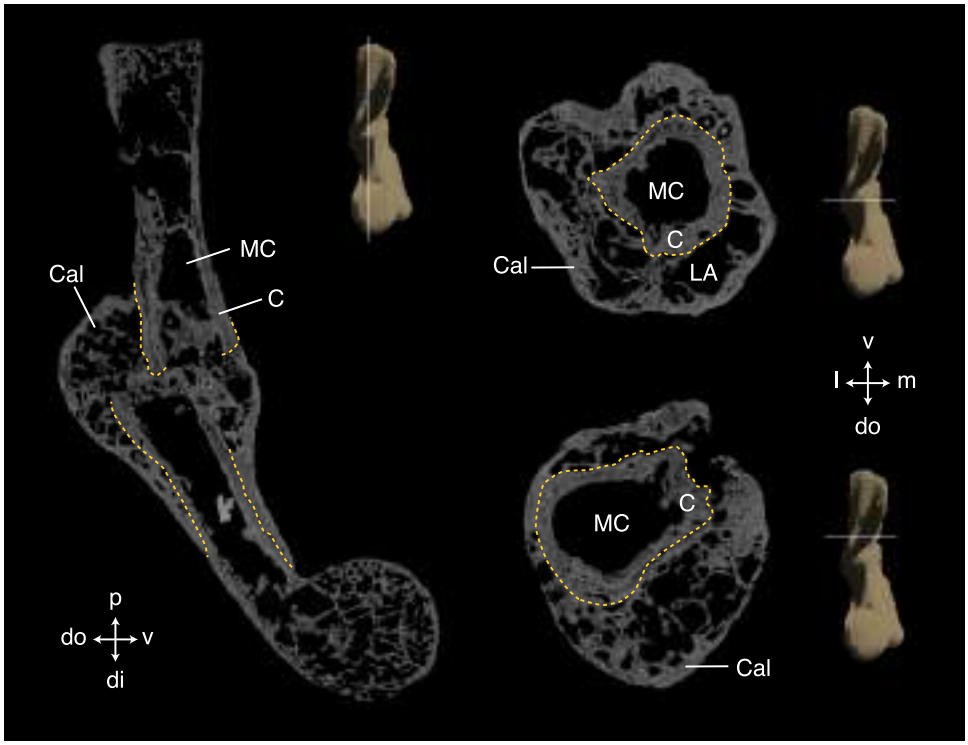


Figure 2 MicroCT images of *Latonia* sp., IPS15200, right humerus. In the left, parasagittal section; and in the right, transversal sections. The exact point of the section is marked by cutting lines in the miniatures. The dashed lines split the healthy cortical bone from the hard callus. Abbreviations: C = cortical, Cal = callus, di = distal, do = dorsal, l = lateral, LA = lytic area, m = medial, MC = medullary cavity, p = proximal, v = ventral.

the likelihood of the possible diagnoses that remained (Appleby 2022). The listed literature is used for comparative purposes and to achieve a differential diagnosis: Knafo (2019), Meuten (2017), Sanchiz and Pérez (1974), Rothschild (2010), Rothschild and Laub (2013), Skutschas et al. (2018), and Rothschild et al. (2023).

Paleopathological disorders in extinct relatives: literature review

For reaching the most likely differential diagnosis, comparison of fossil lesions with those of extant phylogenetically close relatives/analogs is essential (Witzmann and Asbach 2022; Rothschild et al. 2023). However, it is also of relevance to know what kind of disorders have been documented and diagnosed in extinct-related species, in order to highlight the uniqueness of some of them. Refer to Supplementary Table S1 for an exhaustive review of the literature on injuries and disorders reported and diagnosed in extinct anurans, lepidosaurs, and ruminants.

Results

Order Anura Fischer von Waldheim, 1813
Family Alytidae Fitzinger, 1843
Genus *Latonia* von Meyer, 1843
Latonia sp.

IPS15200: humerus

Right humerus, with the main diagnostic elements preserved (e.g., *eminentia captitata*, *crista medialis*) (Fig. 1a). In the mid-region of the diaphysis, an anomalous bone growth is located, with a rough and porous surface. Along the proximo-distal axis, the bone has suffered a marked angulation (approximately 20°), causing the proximal end to shift toward the ventro-medial region. The bone has an external shortening and deformed aspect, yet robust. The deformation also affects the morphology of several elements, such as *crista paraventralis* and *crista ventralis*, which are truncated.

Consistent with the external macroscopic description, the study of the internal microstructure of the bone allows us to observe an interrupted diaphysis with a large displacement (Fig. 2, Supplementary Media S1). Around the 2 broken bone extremities, a large mineralized callus of reactive bone is present, evidencing fracture repair and potential remodeling. The bone density in the affected area is similar to that of healthy bone. The macroscopic study and the internal microstructure revealed a fracture with malaligned healing. In addition, extensive lytic areas (large voids) are identified in the hard callus, which drained externally through a sinus tract. This suggests a probable infectious condition secondary to the trauma. The cartilaginous callus is formed approximately 2 months postfracture, and the formation of a hard callus takes slightly longer (Pritchard and Ruzicka 1950) indicating that this specimen likely survived for at least several months after the injury occurred.

IPS15748: femur

Left femur, with a diaphysis completely preserved and with both epiphyses broken (Fig. 1b). In the proximal region, the medullary cavity is exposed, whereas the remains of the cancellous bone are observed in the distal region. Pathogenic bone

Downloaded from academic.oup.com/cz/advance-article/doi/10.1093/cz/zoag023/8556684 by guest on 23 October 2026

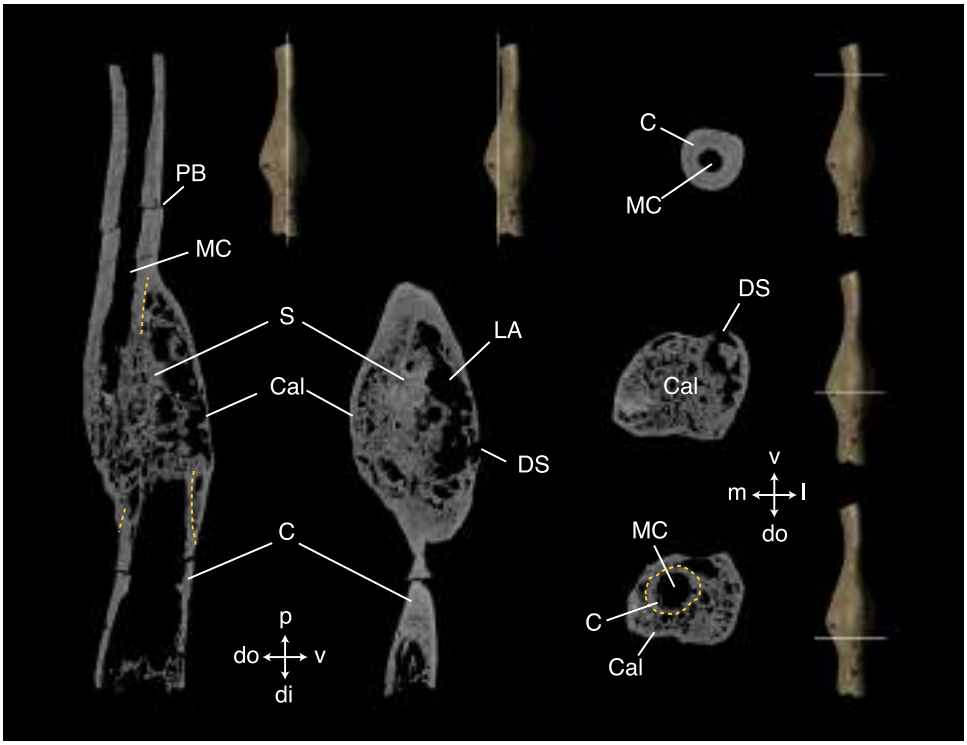


Figure 3 MicroCT images of *Latonia* sp., IPS15748, left femur. In the left and middle, parasagittal sections; and in the right column, 3 transversal sections. The exact point of the section is marked by cutting lines in the miniatures. The dashed lines split the healthy cortical bone from the hard callus. Abbreviations: C = cortical, Cal = callus, di = distal, DS = draining sinus, do = dorsal, l = lateral, LA = lytic area, m = medial, MC = medullary cavity, p = proximal, PB = postmortem break, S = saucerization, v = ventral.

growth is identified in the mid-region, closer to the distal end, and affects approximately 40% of the remain. Its surface is smooth but features some deep holes (see below) and has a sturdy appearance. The healthy ends of the diaphysis are not correctly aligned in the lateral view, indicating considerable displacement. In addition, postmortem fractures are present in healthy regions, likely related to fossildiagenetic processes.

The observation of the internal microstructure of IPS15748 revealed 2 diaphyseal fragments separated by a wide gap (displacement), as the macroscopic examination had suggested. Surrounding these broken ends, a large hard callus of reactive bone was formed, associated with fracture repair and likely remodeling. The bone density in the callus is similar to that in the healthy zones (Fig. 3, Supplementary Media S2). This malaligned healing suggests a fracture caused by a severe trauma. A significant infection (osteomyelitis) occurred during the healing process, evidenced by the pores (draining sinus or cloacae) in the callus surface and the large lytic areas (resorption areas) within it. The remodeling around the large pores rules out a vascular origin for them. The largest draining sinus is visible in ventral view, in the lateral region of the callus (Fig. 1b). In addition, in the proximal end, regions showing reduced or increased bone density were observed. The most significant one is a surface saucerization accompanied by a wide transition zone and a second drainage pathway to the surface. As suggested in IPS15200, this specimen likely survived for at least several months after the trauma, though it probably had an abnormal posture.

IPS16079: undetermined long bone

Diaphysis of an undetermined long bone, with medullary cavities exposed at both ends (Fig. 1c). The epiphyses are not preserved, along with its fragmentary nature and severe pathological condition, precludes specific anatomical identification. Postmortem fractures are evident on the surface of the specimen. Approximately 90% of the fragment is irregularly expanded, while both ends have a macroscopically normal appearance. The surface is rough and grainy and features both small and very large pits (spheroid defects). Some of these spheroid defects exhibit sclerotic edges and form clusters, resembling “brass knuckles”. These lesions are similar, though not identical, to those associated with actinomycosis infection (Rothschild et al. 2006).

Radiologic examination of IPS16079 reveals 2 misaligned diaphyseal fragments, surrounded by new bone, forming a hard callus (Fig. 4, Supplementary Media S3). Reactive bone formed around the fractured regions unites them. A significant angulation (approximately 30°) between the 2 fragments, accompanied by overlap, is observed. This indicates shortening of the bone, which likely impacted and compromised the locomotor functions of the individual. However, one of the ends has the medullary cavity (breaking point end) still exposed to the external surface, corresponding to one of the large pits identified during external macroscopic examination (Fig. 4). These findings suggest the individual experienced a significant trauma. Although some radiolucent areas resemble those associated with actinomycosis, the presence

Downloaded from academic.oup.com/cz/advance-article/doi/10.1093/cz/zoag023/8556684 by guest on 23 October 2026

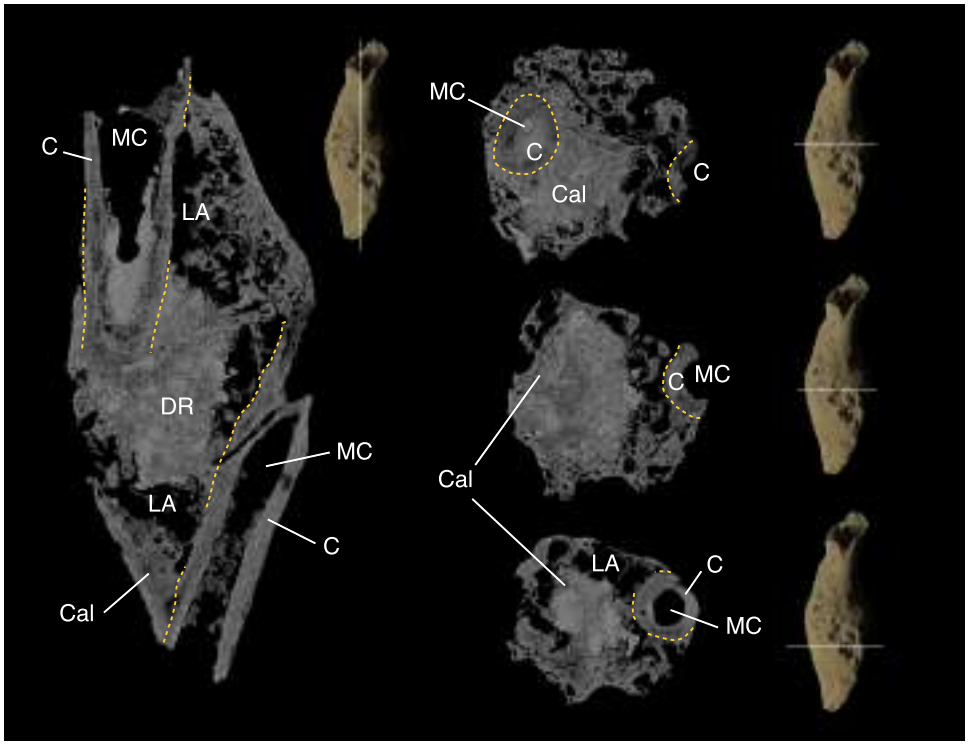


Figure 4 MicroCT images of *Latonia* sp., IPS16079, undetermined diaphysis of a long bone. In the left, longitudinal section; and in the right column, 3 transversal sections. The exact point of the section is marked by cutting lines in the miniatures. The dashed lines split the healthy cortical bone from the hard callus. Abbreviations: C = cortical, Cal = callus, DR = dense region, LA = lytic area, MC = medullary cavity.

of well-defined, variably shaped densities within the mass excludes that diagnosis (Rothschild et al. 2006). None of the densities exhibits the form of sclerotic arcs; instead, they present an almost popcorn-like appearance. However, their thickness exceeds what is typically observed in cartilage neoplasms, such as chondrosarcoma (Resnick et al. 2002; Gazendam et al. 2023). The evidence supports a diagnosis of osteomyelitis (an infectious disease of bone characterized by osteolysis and periosteal reactions). This condition likely developed secondary to a trauma resulting in a compound fracture, defined as a fracture in which the overlying skin integrity is compromised.

IPS16080: tibiofibula

Right tibiofibula, with distal epiphysis and part of the diaphysis preserved (Fig. 1d). Some diagnostic features are observed (including *sulcus distalis*, tibial and fibular distal condyles). Part of the medullary cavity is exposed at the proximal end of the fibula (anterior view), resulting from erosion and postmortem breakage. Several diagenetic fractures are noted in the diaphysis near the nutrient foramen (posterior view). In lateral view, a severe angulation is observed between the proximal and distal ends (approximately 20–30°), though it does not suggest significant displacement (at least in the proximal–distal projection). Anomalous bone growth is identified in the mid-region of the specimen, with numerous pits and holes (some of which are filled with sediment). Due to the state of the specimen, it is suggested that some of these features are a consequence of erosion and do not have a pathological origin.

An interrupted diaphysis joined by thin trabeculae is observed in the microstructural images (Fig. 5, Supplementary Media S4), consistent with a pathologic fracture. Massive reactive bone embeds both extremities, and the mid-region appears solid and robust. The mineralized hard callus is porous and contains lithic areas, some of which open to the exterior via sinuses with non-angular margins (not related to erosion), suggesting a secondary infection (osteomyelitis). The presence of fragile trabeculae of regular thickness (cancellous bone) in the center could associate it with a secondary fracture resulting from osteosarcoma (Rothschild et al. 2018). However, the absence of detectable differences in bone density between healthy and reactive bone along with the large gap between corticals (Fig. 5) is consistent with a traumatic fracture, which is likely the most probable diagnosis.

IPS16081: undetermined long bone

Diaphysis of a long bone, likely a right femur (see *crista femoris*), with the medullary cavity exposed at both ends (Fig. 1e). The specimen consists of a diaphysis (proximal end, approximately 2 cm) attached to an anomalous, shapeless growth. An angulation of 25–30° between the residual diaphysis on both sides of the bone overgrowth is observed. Although cortical bone loss of variable size and shape is present, it is unclear whether these surfaces were intact pre-mortem. The irregular character of defect edges suggests taphonomic effects (postmortem surface breakage). Lobular new bone formation is identifiable within the defects.

CT examination reveals an expansile, lytic process with large struts, areas displaying an irregular pattern of trabeculae with variable thickness (upper area of figure), and a zone of curvilinear, thick radiodense material at its upper surface, just below the angulation (Fig. 6, Supplementary Media S5). The bone at

Downloaded from academic.oup.com/cz/advance-article/doi/10.1093/cz/zoag023/8556684 by guest on 23 October 2026

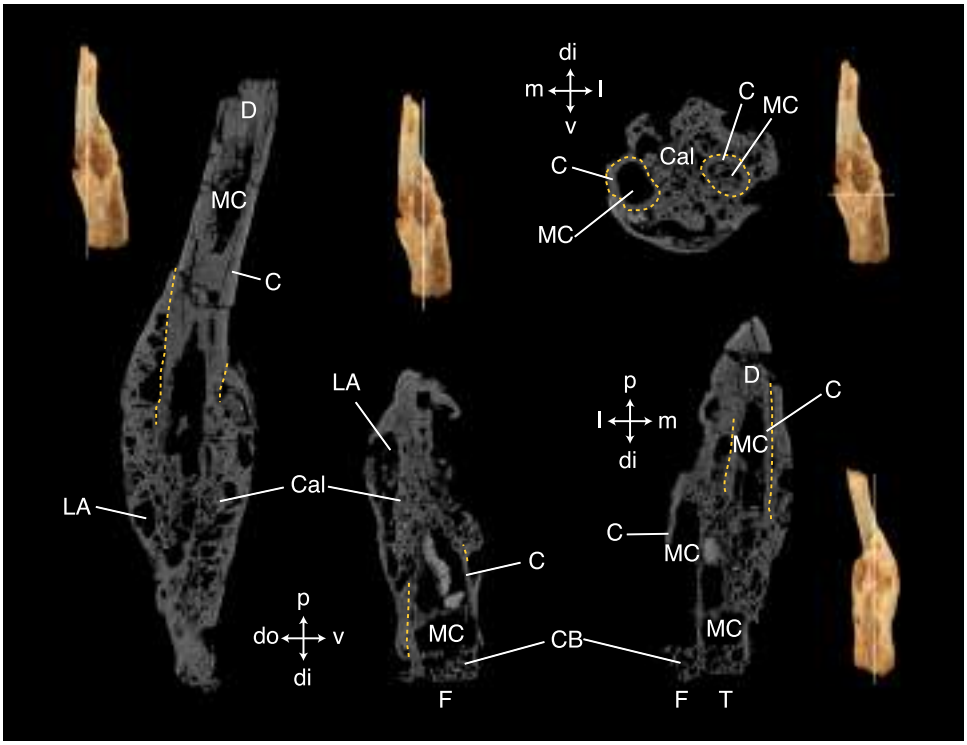


Figure 5 MicroCT images of *Latonia* sp., IPS16080, right tibiofibula. In the 2 left columns, parasagittal sections; top right corner, transversal section, and bottom right corner, frontal section. The exact point of the section is marked by cutting lines in the miniatures. The dashed lines split the healthy cortical bone from the hard callus. Abbreviations: C = cortical, Cal = callus, CB = cancellous bone, D = diaphysis, di = distal, do = dorsal, F = fibula, l = lateral, LA = lytic area, m = medial, MC = medullary cavity, p = proximal, T = tibia, v = ventral.

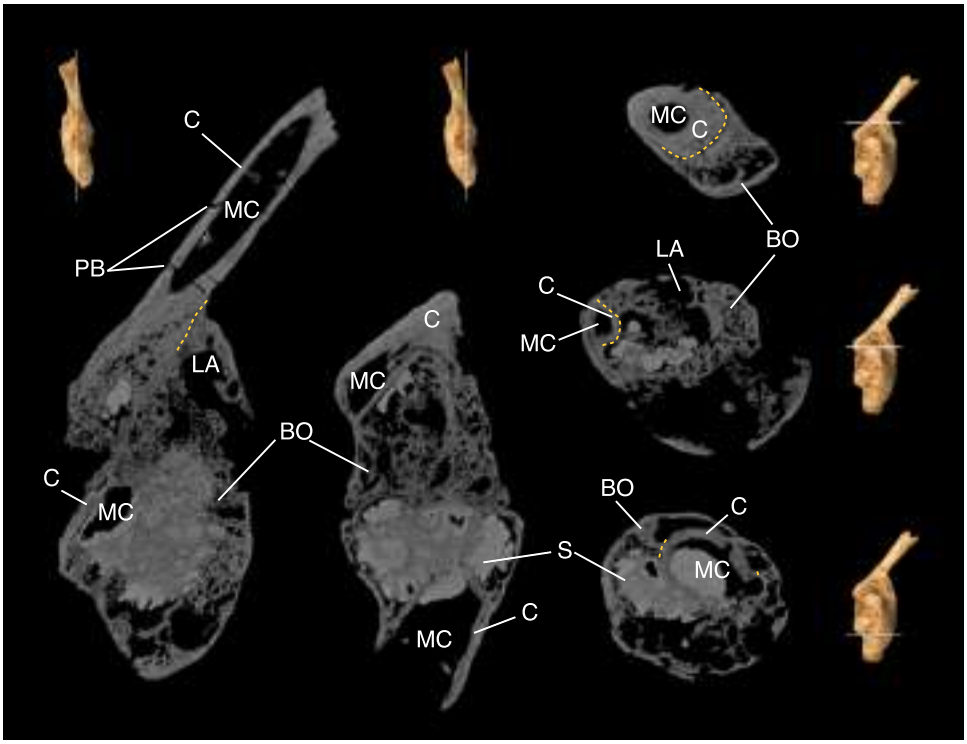


Figure 6 MicroCT images of *Latonia* sp., IPS16081, long bone (?right femur). In the 2 left, longitudinal sections; and in the right, transversal sections. The exact point of the section is marked by cutting lines in the miniatures. The dashed lines split the healthy cortical bone from the hard callus. Abbreviations: BO = bone overgrowth, C = cortical, LA = lytic area, MC = medullary cavity, PB = postmortem breakage, S = sediments.

Downloaded from academic.oup.com/cz/advance-article/doi/10.1093/cz/zoag023/8556684 by guest on 23 October 2026

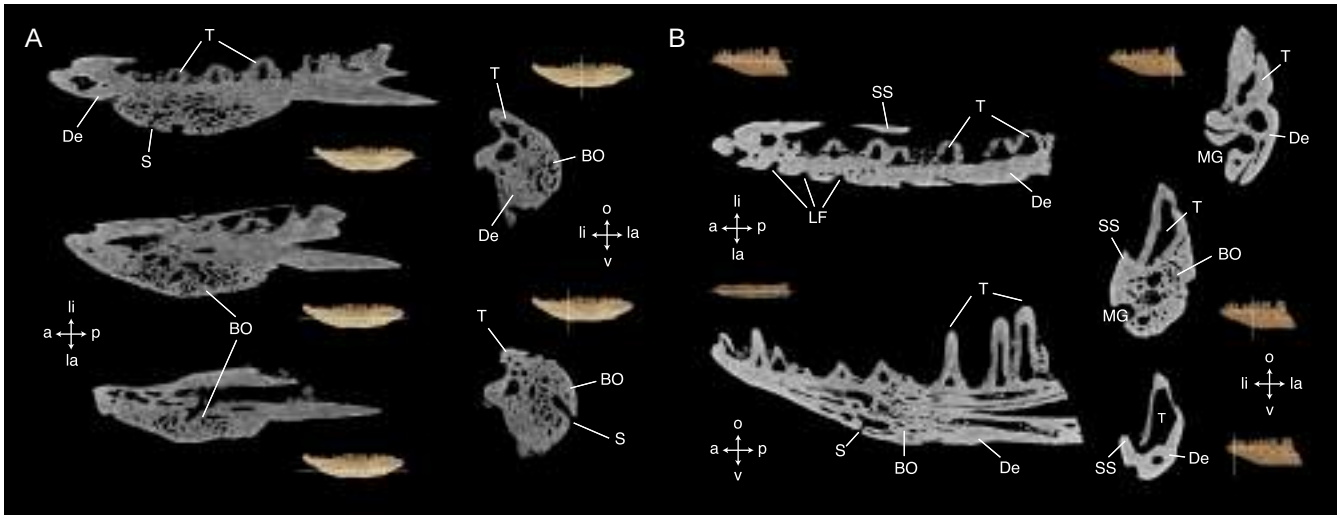


Figure 7 MicroCT images of *Podarcis lilfordi*: a) CBQ-368a, left dentary. In the left column, frontal sections; in the right one, transversal sections; b) CBQ-368b, left dentary. In the top left corner, frontal section; in the bottom left corner, parasagittal section; and the right column are transversal sections. The exact point of the section is marked by cutting lines in the miniatures. Abbreviations: a = anterior, BO = bone overgrowth, De = dentary, la = labial, li = lingual, LF = labial foramina, MG = Meckelian groove, o = occlusal, p = posterior, S = sinus, SS = subdental shelf, T = teeth, v = ventral.

the angulation is abnormal, indicating a pathologic fracture. Additionally, the upper portion of the lower aspect of the images contains a mass of variable density, apparently containing abnormal irregular trabeculae. The abnormal trabecular pattern and severe cortical thinning suggest an osteosarcoma, whereas the struts and large cavernous spaces are consistent with an aneurysmal bone cyst (ABC). ABCs consist of multiloculated blood-filled spaces enclosed by reactive bone. Most are located in the metaphyses. They may be a primary bone lesion, but are often secondary, arising as complications of primary bone neoplasms. However, the diaphyseal location suggests the possibility that the underlying disease was a telangiectatic osteosarcoma (high-grade malignant neoplasm).

Order Squamata Oppel, 1811
Family Lacertidae Gray, 1825
Genus *Podarcis* Wagler, 1830
Podarcis lilfordi Günther, 1874

CBQ-368a and CBQ-368b: dentaries

Left dentaries, with anterior region intact and posterior part missing, including the coronoid and angular processes, splenials, and articular bones, among others (Fig. 1f and 1g). The pleurodont dentition is mostly intact, except for some lost and broken teeth. The subdental shelf and Meckelian groove are clearly identified in the CBQ-368a specimen (lingual view) but are partially obscured in CBQ-368b. Labial foramina are observed in both individuals, with a greater abundance in CBQ-368b. CBQ-368a exhibits an external protuberance on the labial side, affecting the dentary at the location of the 5th to 13th teeth (counted from anterior). This anomalous bone growth has a granular appearance and is perforated with pits of varying sizes. This region of the dentary appears curved and hypertrophied in occlusal view. CBQ-368b displays pathological bone on the inner side of the dentary, at the level of the 7th to 12th teeth. The subdental shelf is elevated compared to healthy areas and has a smooth appearance, with 3 large pores. A fine layer of anomalous bone growth is observed over the labial aspect of the dentary. Occlusal view reveals a protruding, deformed bone.

CT sections of the condition in CBQ-368a reveal destruction of the outer cortical layer with irregular subperiosteal new bone formation composed of thick trabeculae, showing similar bone density to the surrounding normal bone (Fig. 7a, Supplementary Media S6). Focal areas of resorption are noted in these trabeculae, forming sinus cavities with drainage to the exterior. This is consistent with a diagnosis of infection complicated by fibresceses (fibrous abscesses). The microstructure of the pathological region of CBQ-368b is similar to that reported in CBQ-368a (Fig. 7b, Supplementary Media S7). The lingual region additionally exhibits a solid appearance (without holes). Enlarged chambers on the ventral aspect contain drainage canals, suggesting sinuses connecting externally. These sinuses are unrelated to the lingual, alveolar, or mylohyoid foramina. These observations are consistent with a diagnosis of infection complicated by fibresceses (fibrous abscesses).

Order Artiodactyla Owen, 1848
Family Bovidae Gray, 1821
Genus *Myotragus* Bate, 1909
Myotragus balearicus Bate, 1909

CBQ-928: lower incisor

Lower incisor (i1) (Fig. 1h) with measurements (maximum length of 3.57 cm, maximum width of 0.73 cm) consistent with a permanent tooth of a young adult. The occlusal section is oval-shaped and remains relatively uniform along the entire length of the tooth, without the gradual constriction typical of milk dentition. Dental wear is uniform on all sides of the occlusal view, contrasting with the common wear pattern of artiodactyl incisors (labial side typically less worn than the lingual side due to tooth position, orientation, and materials). Hence, the tooth was extensively used. Enamel is only present on the labial side, a feature observed in *M. balearicus* and other species (e.g., vicuña and

Downloaded from academic.oup.com/cz/advance-article/doi/10.1093/cz/zoag023/8556684 by guest on 23 October 2026

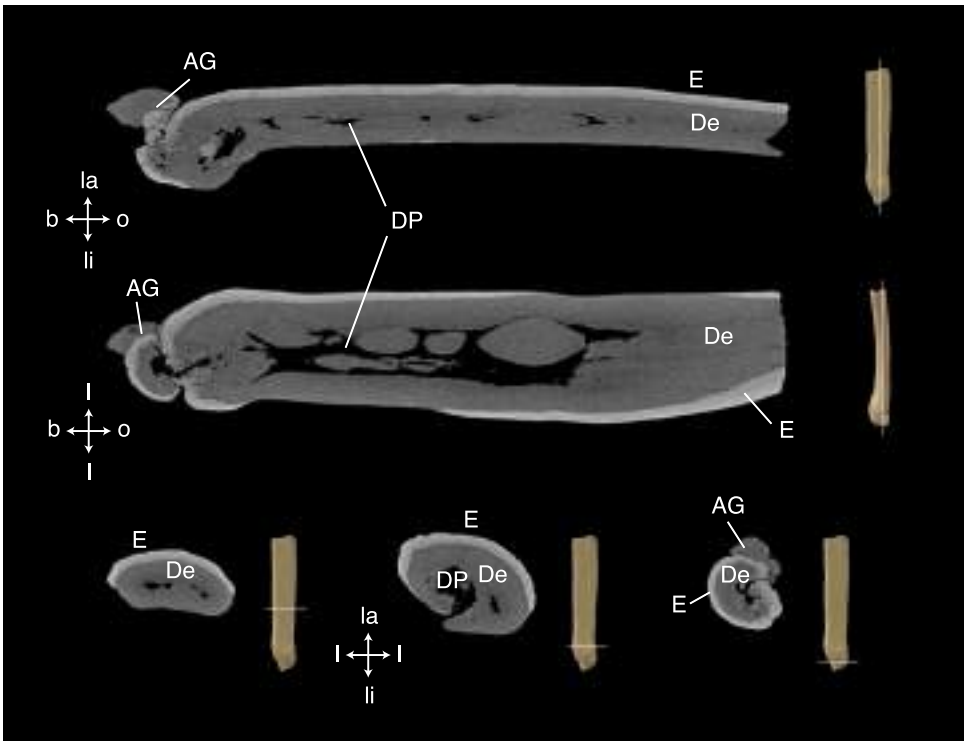


Figure 8 MicroCT images of *Myotragus balearicus* CBQ-928, lower permanent incisor 1 (i1). In the top, sagittal section; in the middle, transversal section, and in the bottom, frontal sections. The exact point of the section is marked by cutting lines in the miniatures. Abbreviations: AG = anomalous growth, b = basal, De = dentin, DP = dental pulp, E = enamel, l = lateral, la = labial, li = lingual, o = occlusal.

rodents). The thick enamel coat covering the entire labial side is characteristic of permanent incisors, contrasting with deciduous teeth (Andrews 1915; Bover and Alcover 1999). A slight channel can be observed on the lingual side. Other significant traits, such as the slight spiral torsion, have not been clearly observed and may be obscured by the pathological condition. The first incisors of *M. balearicus* are rodent-like, ever-growing, with open roots (coined as elodont or rootless). In contrast, CBQ-928 lacks an open root. Instead, there is a torsion of the tooth itself, and an anomalous shapeless growth on the labial region, external to the tooth's structure. Whereas the surface of the tooth is smooth, the anomalous growth is rugose and contains several grooves.

The microstructural analysis distinguishes enamel and dentin easily on both the labial and lingual sides (Fig. 8, Supplementary Media S8). The dental pulp is discontinuous and obstructed by dentin bodies. In addition to a twisting of the tooth itself (with enamel surrounding the entire tooth at certain basal points), there is a constriction that separates a small terminal section of the tooth along with a labial dentin amalgam. The root is completely closed, preventing the continuous growth of the tooth. Its morphology is irregular, not resembling the rooted incisors of other bovids. The absence of an open root led to excessive wear of the tooth, consistent with the occlusal section of CBQ-928. The status of the other incisors and teeth in the specimen is indeterminate, but malocclusion and subsequent feeding complications were likely. Considering the available evidence, the most probable cause of this abnormality is a late-onset congenital malformation or fracture (though microstructural images do not provide conclusive evidences). However, the absence of the jaws and the remaining dentition prevents a more confident diagnosis in this case.

CBQ-SN: rib

Right rib, with proximal end (head, neck, and tubercle) and part of the distal region (rib body with costal groove in medial view) (Fig. 1i). The rib number could not be determined. In lateral view, significant erosion is observed in the neck-tubercle region. The rib body is broken at the distal end, and the sternal extremity is missing, exposing the cancellous bone. The surface exhibits disruptions and grooves resulting from fossildiagenetic processes. Lateral view also reveals swelling at the rib's distal aspect, with surface disruption characterized by grooves and residual pores.

Bone overgrowth is identified in the most anterior lateral margin of the rib, clearly visible in parasagittal sections (Fig. 9, Supplementary Media S9). Cortical thinning is observed in the neck of the rib. The distal end is characterized by a disrupted cortex with a saucer-like depression, covered by a perforated periosteal shell. Saucerization, excavation of the outer cortical margin of bones, can result from soft-tissue masses (such as lymphadenopathy, aneurysms, pigmented villonodular synovitis, foreign body granulomas, bronchogenic carcinoma, and Ewing's sarcoma). Osteomyelitis has occasionally been listed as a potential cause of saucerization (really, it is a product of medical intervention, not an inherent manifestation of the osteomyelitis) (Shannon et al. 1973). There is, however, one infectious entity that does actually produce saucerization: the tropical (Bureli) ulcer. Although the tropical ulcer could be considered a variety of osteomyelitis, its manifestations are quite distinct from the usual characterization of that phenomenon (Resnick 2002; Micheletti Cremasco et al. 2015). On the other hand, the presence of periosteal reaction in CBQ-SN excludes simple soft

Downloaded from academic.oup.com/cz/advance-article/doi/10.1093/cz/zoag023/8556684 by guest on 23 October 2026

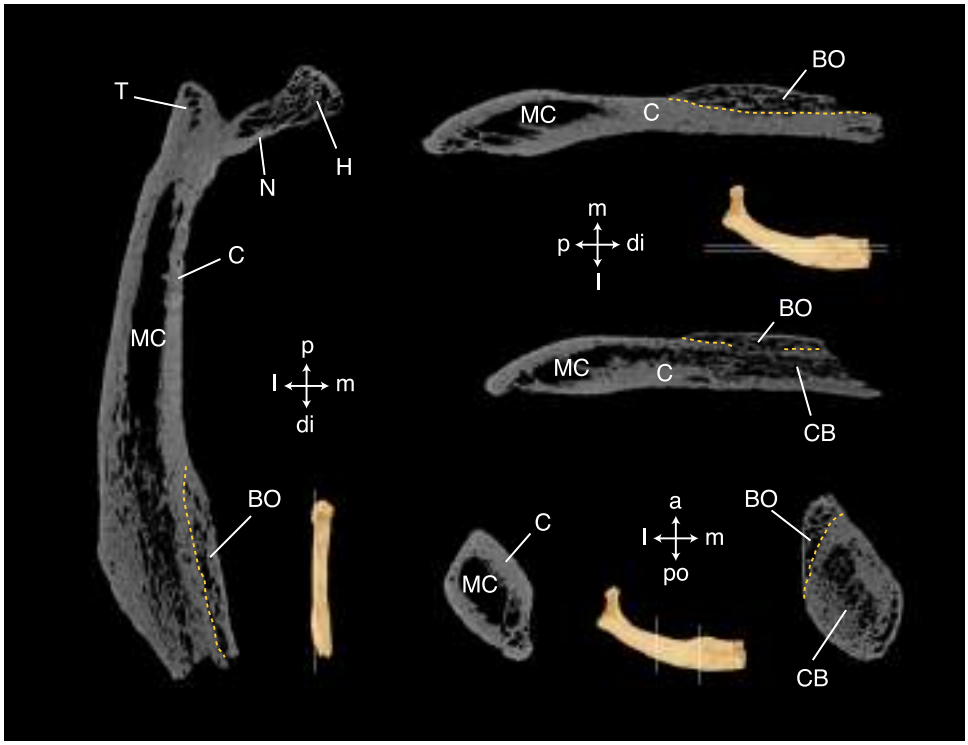


Figure 9 MicroCT images of *Myotragus balearicus* CBQ-SN, right rib. In the left, transversal section; in the top right, coronal sections; and in the bottom right, parasagittal sections. The exact point of the section is marked by cutting lines in the miniatures. The dashed lines split the healthy cortical bone from the bone overgrowth. Abbreviations: a = anterior, BO = bone overgrowth, C = cortical, CB = cancellous bone, di = distal, H = head, l = lateral, m = medial, MC = medullary cavity, N = neck, p = proximal, po = posterior, T = tubercle.

tissue mass effect, leaving Ewing's sarcoma and a metastatic bronchogenic carcinoma as diagnostic considerations. The rib would be most atypical for Ewing's sarcoma, and multiple surface disruptions are at variance with metastatic disease. Therefore, most likely explanation is bronchogenic carcinoma.

CBQ-1888: undetermined long bone

Diaphysis of a long bone, with the medullary cavity exposed at both ends (Fig. 1j). The absence of characteristic features in the fragment precludes specific anatomical identification. There is a gradual enlargement of abnormal bone toward one end, which also differs in texture and color from healthy bone. The overgrowth at this end shows a rugose surface, with transverse, predominantly superficial grooves (likely vascular) and multiple perforations. Transverse and cross-sectional views of the pathological end reveal a gap between the affected cortical bone and the overgrowth, transitioning to a loss of separate definition.

The original cortex is not disrupted on CT examination, but is encircled by a disorganized, apparently bony mesh of fine trabeculae (Fig. 10, Supplementary Media S10). The abnormal area surrounding the ectocortical surface differs in character and density from the cortex itself. It is quite porous, and the structures contained within appear to be less dense than the cortical bone. The inferior aspect (on the image) reveals "initiation" of the process with the radiodense elevation characteristic of Codman's triangle. The image also reveals a mass structure surrounded by, but separated from, the surrounding cortical bone by a radiolucent zone. The mass has a honey-comb appearance (unless it is an artifact) that is characteristic of angiomatous neoplasms (both benign and malignant and for lymphangiomas), though popcorn-like neoplasms in chondrosarcoma can also have this aspect. The major differential considerations are forms of osteosarcoma, Ewing's sarcoma, and osteomyelitis. Ewing's sarcomas are characterized by poorly defined margins with a wide zone of transition, in contrast to the sharply defined anomaly in this specimen. Although there are perforations, they seem associated with vascular channels, a phenomenon more commonly linked to neoplasia. The major diagnostic issue is the degree of separation of the neoplasia from underlying bone. Parosteal osteosarcomas are fully separated by a radiolucent line, whereas periosteal osteosarcomas may grow along the bone surface, though such separation is not initially observed. Therefore, a periosteal osteosarcoma is suggested as the most probable diagnosis.

Discussion

Paleopathology primarily deals with diseases that have a skeletal or dental expression, since soft tissues or other remains in which illness could be identified are scarce or rarely preserved in the fossil record (e.g., coprolites or trackways) (Grauer 2022; Rothschild et al. 2023). Skeletal reactions can be very slow processes, taking up to a decade or more to develop in some disorders, and not all diseases leave detectable traces on the hard skeleton of organisms (Wood et al. 1992). Therefore, there is a significant bias between the total number of diseases that

Downloaded from academic.oup.com/cz/advance-article/doi/10.1093/cz/zoag023/8556684 by guest on 23 October 2026

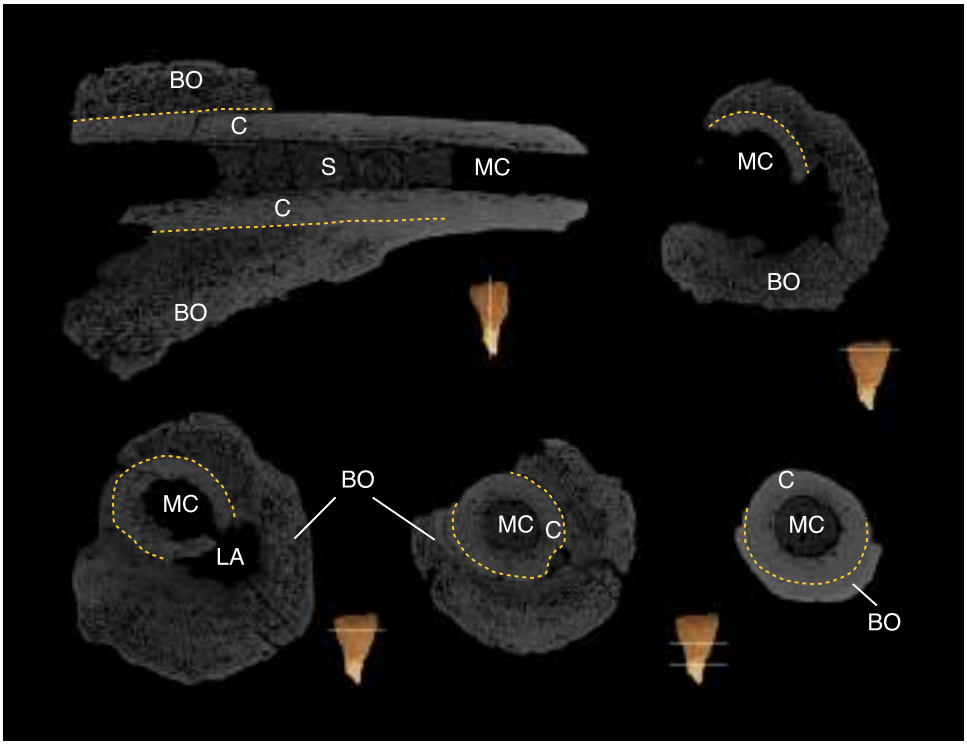


Figure 10 MicroCT images of *Myotragus balearicus* CBQ-1888, diaphysis of long bone. In the top left corner, longitudinal section; in the top right corner and bottom, transversal sections. The exact point of the section is marked by cutting lines in the miniatures. The dashed lines split the healthy cortical bone from the bone overgrowth. Abbreviations: BO = bone overgrowth, C = cortical, LA = lytic area, MC = medullary cavity, S = sediments.

species suffered in the past and those that we can observe and recognize in the fossil record (Witzmann et al. 2021). Additionally, the process of fossilization itself (taphonomy) can obscure or mimic paleopathological reactions (through weathering, transport, abrasion, trampling, etc.) (Wolff 2007). Upon reviewing the literature, paleopathological conditions are more commonly reported in large-sized organisms (e.g., dinosaurs, mosasaurs, and large mammals) (Grauer 2022; Rothschild et al. 2023). This may be the result of a complex set of factors, ranging from (1) small organisms generating less scientific interest (in general, their remains are less studied or only some elements are of interest, e.g., teeth); (2) their relatively brief lifespans (reduce the time and likelihood of developing a disorder); to (3) the added difficulty of observing, identifying anomalies and lesions, and reaching a diagnosis in small-sized elements (especially challenging without the use of microscopic imaging techniques), among other factors (Moncunill-Solé et al. 2019, 2024). For all these reasons, the discovery of paleopathological remains, especially of certain taxa, is always a remarkable finding. In this study, we report and assess 10 vertebrate remains from Menorca exhibiting abnormalities, and propose the most probable diagnoses, including traumatic injuries, neoplastic diseases, infections, and congenital disorders. Several studies have analyzed vertebrate remains from this island, but none of them had previously described paleopathological conditions in these bones or teeth. Therefore, the findings analyzed in the present study hold particular significance, as they are the first documentation of anomalies in *Latonia* and *P. lilfordi*, and the first identification of neoplasms in *Myotragus*, which lived in Menorca during the Plio-Holocene.

Etiology, occurrence, and impact of the disorders

Latonia is currently an endemic monospecific genus (*L. nigriventer*) of Lake Hula marshes (Biton et al. 2013). However, in the past (late Oligocene-Holocene), it was distributed across central and southern Europe, with several occurrences in the Late Pliocene and Pleistocene in France, Germany, Hungary, Italy, Slovakia, and possibly Ukraine (see review in Sorbelli et al. 2025). Most of the lesions observed in the fossil specimens from Menorca (particularly IPS15200, IPS15748, IPS16079, IPS16080; Figs. 1a–d and 2–5) are compatible with fractures resulting from traumatic events. Fractures and amputations of limbs are commonly observed in current and extinct frogs, although the incidence of injury is around 5% in natural populations (Špinar 1972; Sanchiz and Pérez 1974; Ippen and Heinrich 1977; Gray et al. 2002; Rothschild and Laub 2013; Supplementary Table S1). None have been previously reported in either past or extinct *Latonia* individuals (Perl et al. 2017). The sources of traumatic injuries in amphibians are diverse, ranging from sublethal predation events, the result of fighting with conspecifics, mechanical accidents, metabolic bone diseases, and scarring from infections, among others (Gray et al. 2002 and references therein). In the case of the present *Latonia* specimens, considering the fossil material, their environment, and coexistence with other species, mechanical accidents and fighting with conspecifics seem the most probable cause (e.g., males exhibit a well-developed *crista ventralis*, as observed in IPS15200, and their territorial combats involved the use of their forelimbs). Although the difficulties that fractures can entail (in locomotion, normal position,

Downloaded from academic.oup.com/cz/advance-article/doi/10.1093/cz/zoag023/8556684 by guest on 23 October 2026

acquisition of food, mating, etc.), the formation of a hard callus (after more than 2 months) rules out that these specimens died at the time the fracture occurred (Pritchard and Ruzicka 1950; Grauer 2012). In some cases, the analyzed fractures were subsequently contaminated by pyogenic infectious agents, causing nonspecific infectious disease. Osteomyelitis has been briefly reported in extant and extinct anurans, and it can cause symptoms such as local swelling or reduced range of motion (Ippen and Heinrich 1977; Rothschild and Laub 2013).

On the other hand, though teratologies are common disorders in amphibians (Sanchiz and Pérez 1974; Rothschild 2009; Rothschild and Laub 2013; Rothschild et al. 2013), we did not report this kind of abnormality in the analyzed sample, possibly as a consequence of the poor and fragmentary material (Witzmann et al. 2021). However, we identified a rare neoplastic condition, consistent with telangiectatic osteosarcoma, in one of the individuals (IPS16081; Figs. 1e and 6), for which we were unable to determine either the origin or its level of aggressiveness and fatality. Neoplasms are not common in amphibians, especially in wild populations, and none has been previously evidenced in *Latonia* specimens (Perl et al. 2017; Albuquerque et al. 2018). The most frequent ones (Lucke renal carcinoma and the benign squamous cell papilloma) typically do not leave traces on the skeleton (Densmore and Green 2007). Few cases of spontaneous bone neoplasm have been cited in the literature, though later examinations of some of them have revealed misdiagnoses (Olmacher 1898; Schlumberger and Lucke 1948; Green and Harshbarger 2001; Densmore and Green 2007; Rothschild and Laub 2013). The incidence of neoplasia is higher in captive individuals, who are protected from natural threats like predation and environmental hazards, and, accordingly, the number of reported cases has increased significantly in recent years (Green and Harshbarger 2001). Consequently, the diagnosis proposed for IPS16081 represents a highly atypical condition in wild populations.

The genus *Podarcis* currently has a circum-Mediterranean distribution (southern Europe, Anatolian Peninsula, and northern Africa) with approximately 25 species (Speybroeck et al. 2020). In the past, it was hypothesized to have been widely present throughout Europe from the Zanclean onwards, although caution is required because most fossil identifications were based primarily on biogeographic considerations (Villa and Delfino 2019). The 2 abnormalities recognized in the Menorca jaws of *P. lilfordi* specimens are compatible with an infection complicated by fibrous abscesses (CBQ-368a and CBQ-368b; Figs. 1f–g, 7). Pyogenic and other types of infections are commonly described in extant reptiles (particularly, in captive specimens) (Rothschild et al. 2013) and have also been observed in extant *Podarcis* spp., although without affecting the bones (Storniolo et al. 2022; Faria et al. 2024). Their origins are related to trauma, stress, or immunocompromise, and subsequent opportunistic colonization of the microbial organisms, which generally arrived from the flora and environment (such as *Mycobacterium*) (Knafo 2019). Trauma and secondary infection of the jaw are frequent in lizards, though no primary fracture was visible in our material (Fig. 7). Depending on the conditions and the magnitude of the disease, bony infections can become systemic and fatal. However, in reptiles, the lytic lesions resulting from infection can persist long after the disease has been cleared (Knafo 2019). Therefore, we cannot determine if *P. lilfordi* specimens suffered this condition before their death, or if the infection was active at the time of death.

On another front, *Myotragus balearicus* is an extinct species with a very restricted distribution (Mallorca and Menorca). The closest extant relative of this species is the takin (*Budorcas taxicolor*), a caprine from the eastern Himalayas (Bover et al. 2019). Two of the 3 studied remains of *M. balearicus* are interpreted as exhibiting neoplastic lesions, consistent with bronchogenic carcinoma (CBQ-SN, Figs. 1i and 9) and periosteal osteosarcoma (CBQ-1888, Figs. 1j and 10). Studies on neoplasms in ruminants (including bovids) are rarely reported in the literature, particularly concerning wild populations; with the integumentary system being the most commonly affected (Meuten 2017; Vasconcelos et al. 2023). The origin of neoplasms is generally unknown, and several factors (e.g., genetics, injuries, etc.) can predispose specimens to develop them (Meuten 2017). Pulmonary neoplasia is not common in domestic animals, with most cases being adenocarcinoma and pulmonary blastoma (aggressive type) in bovines. In this group, the incidence is approximately 2–20 cases per million (Wilson 2017). The bone metastasis of lung cancers commonly involves the ribs, spine, pelvis, and other bones. The arrival of neoplastic cells at the surface of the bone disrupts the normal bone reconstruction, leading to tissue destruction and osteolytic lesions (Wu et al. 2021). This type of carcinoma is not generally observed in young specimens: the reported average age is 10.8 years in dogs and 12–13 years in cats (Wilson 2017). On the other hand, primary malignant bone neoplasms (osteosarcoma, chondrosarcoma, fibrosarcoma, and others) are uncommon in domestic animals too (Vasconcelos et al. 2023). Peripheral sarcomas (periosteal and parosteal types) are less aggressive and common (low incidence and prevalence) than those of medullary origin (central ones). They grow at a slower rate, rarely metastasize, and occur at older ages than central osteosarcomas (Thompson and Dittmer 2017). Considering the literature, it is likely that although specimens with periosteal osteosarcoma could live with this condition several times, those with bronchogenic carcinoma and bone metastases have a poorer prognosis.

Finally, we associated the abnormality of the *M. balearicus* tooth (CBQ-928, Figs. 1h and 8) with a possible late-onset congenital malformation or fracture (though no signs of fracture were identified). Tooth anomalies are observed in mammals and mainly consist of deformed or missing cups and crowns, teeth fusion, excessive growth of dentine, and abnormal root morphology, among others (Witzmann et al. 2021). The origin of such malformations can stem from genetic, environmental factors, or a combination of both. The tooth was found in isolation, so we were not able to determine what the rest of the dentition looked like. However, we ruled out this abnormality as a possible case of atavism (reappearance of ancestral traits), as the tooth features of shapeless root with a torsion are far from resembling the normal rooted incisors of bovids. Some teratologies can be lethal or semi-lethal; however, the extensive wear suggested that this incisor was strongly used. In extant ruminant, most congenital malformations involve soft tissues, without traces on the skeleton (Bodinga et al. 2020). Dental malformations and abnormalities are rarely reported in these mammals, although a few cases of shapeless, absent, or supernumerary teeth have been published (Corbera et al. 2017). Few cases of tooth fractures have been reported in adult goats (Canpolat

Downloaded from academic.oup.com/cz/advance-article/doi/10.1093/cz/zoag023/8556684 by guest on 23 October 2026

et al. 2017). In taxa with open-rooted teeth, such as rabbits and rodents, traumatic injuries may damage the apical germinal tissue, affecting normal tooth growth and leading to malocclusion (Capello 2004).

Both type of pathologies (neoplasia and congenital malformations/tooth fractures) are very unusual, as they have not been previously described in *Myotragus* and have been rarely reported in extant and extinct relatives. In addition, these findings expand our knowledge of the lesions and disorders observed in this species, as until now, only bone fractures and undiagnosed cases had been documented (Waldren and Kopper 1968; Alcover et al. 1981; Jordana et al. 2011).

Insularity and disease: an evolutionary perspective

The presence of injuries and lesions in insular extinct vertebrates is not uncommon, with anomalies diagnosed in lagomorphs (Zoboli et al. 2018; Moncunill-Solé et al. 2024), bovids (Waldren and Kopper 1968; Jordana et al. 2011), cervids (Sondaar 1977; Alcover et al. 1981; Dermitzakis et al. 2006; Lyras et al. 2016, 2019; Palombo and Zedda 2016, 2022), and hippopotamids (Maempel 1993; Rothschild et al. 2023), among others. In extant island species, dental and osteopathological disorders have also been documented (Verstraete et al. 1996; Peterson et al. 2010; Brown et al. 2020; Christie et al. 2023). The number of pathological conditions and affected specimens is remarkable in some of these species (e.g., *P. sardus*), particularly when compared to the prevalence and incidence in their extant relatives or to the number of reported cases in extinct mainland populations (see Moncunill-Solé et al. 2024). Additionally, we identified exceptionally rare abnormalities, which occur with very low incidence in their extant relatives (present results; Moncunill-Solé et al. 2024). The 2 key ecological factors of island environments (lower extrinsic mortality and resource limitation) may help explain this phenomenon, grouping the anomalies observed in extinct insular vertebrates into 3 categories:

1. Healed fractures, infections, congenital anomalies, and chronic conditions (long-term health condition that may not have a cure): the manifestation of some paleopathological features (e.g., hard calluses in Menorca *Latonia* specimens) indicates that the individual survived through the disease episode (Grauer 2012), though it may have affected mobility, feeding, or safeguarding abilities. Generally, injured or developmentally abnormal specimens become easier targets for predators. Surviving in this diseased state can be quite challenging in predator-rich mainland habitats. However, on islands, which are typically free of terrestrial predators or where these are present in significantly reduced numbers (Palkovacs 2003), injuries can heal (if immune system provides the appropriate response), or individuals may survive with teratologies or chronic conditions (e.g., *Candiacervus* with pituitary gigantism, *P. sardus* with chronic inflammatory, etc.) (Zoboli et al. 2018; Palombo and Zedda 2022; Moncunill-Solé et al. 2024). Zoboli et al. (2018) suggested that some of these congenital anomalies could be a consequence of the founder effect, genetic drift, or inbreeding in small population sizes of island environments, but these hypotheses have not yet been tested and confirmed.
2. Hypoplasia, osteoporosis, and other malnutrition-related defects: Poor nutrition can impose severe metabolic stress, slowing or interrupting the normal growth of individuals. This can be particularly pronounced in low-energy environments, such as islands. In this context, Brown et al. (2020) documented enamel hypoplasia and other skeletal anomalies in moose populations from Isle Royale (an island similar in size to Menorca), even when the population was not at carrying capacity levels (during peak irruption or resource decline) [see also Peterson et al. (2010) for further discussion on this topic]. Furthermore, they observed an increase in the prevalence when wolf populations were less abundant. In fossil specimens, Sondaar (1977) described osteoporosis in several bones of Pleistocene deer from Crete, associating this condition with mass starvation as a consequence of overpopulation. In this regard, Dermitzakis et al. (2006) evidenced that the deer were affected by an osteopenic bone disease, likely as a consequence of prolonged malnutrition. Also, in the deer from Crete, Lyras et al. (2019) noted that several *Candiacervus* specimens from the Mavromouri caves (Crete) were affected by a severe metabolic bone disease, likely nutritional secondary hyperparathyroidism. Likewise, Alcover et al. (1981) reported 2 populations of *Myotragus* characterized by their particularly small size, shortened horns, and heavily worn teeth, which were interpreted as evidence of malnutrition and periods of food scarcity. On the other hand, Zoboli et al. (2018) also diagnosed osteomalacia in *P. sardus* remains. However, some of these anomalies have not been analyzed in detail at both macroscopic and microscopic levels. To date, hypoplasia and other malnutrition-related defects have not been described in extinct insular species. It is likely that such anomalies have simply gone unnoticed.
3. Age-related or degenerative disorders, such as osteoarthritis and certain neoplasms: In island species, we have identified diseases that are unusual in natural populations or that have only been observed in specimens living in captivity. For example, when examining osteoarthritis in Sardinian *Prolagus*, Moncunill-Solé et al. (2024) discovered that this degenerative condition was present in the island population, but it had never been diagnosed in wild pika populations. The authors noted that its prevalence rate was similar to or higher than that of domestic lagomorphs. The authors linked this condition to the longer lifespan of the species (Fernández-Bejarano et al. 2024). In insular scenarios, natural selection favors traits that maximize lifetime reproduction and lifespan (Palkovacs 2003). As a result, the extended lifespan of insular populations may provide increased time and a greater opportunity for the expression of certain disorders compared to mainland species (in a manner analogous to what has been observed in some species under managed care) (Cagan et al. 2022; Compton et al. 2025). This extended longevity may facilitate the emergence or detection of conditions that are rarely documented in extant natural populations (e.g., neoplasms of *M. balearicus* or *Latonia*). Particularly in amphibians, it has been noted a higher incidence of neoplasms in individuals living beyond

Downloaded from academic.oup.com/cz/advance-article/doi/10.1093/cz/zoag023/8556684 by guest on 23 October 2026

their average lifespan under human care (Compton et al. 2025).

In view of this, the unique selective pressures of islands (lower extrinsic mortality and resource limitation) may promote a higher prevalence of paleopathological conditions in insular species. In addition, Zoboli et al. (2018) highlighted that insular population might suffer from abnormalities related to the inbreeding depression, despite the lack of testing or confirmation for this hypothesis.

Final remarks

To sum up, paleopathological conditions are an invaluable source of information, offering insights into the biology and ecology of extinct species. The examination of remains of insular species from Plio-Holocene deposits of Menorca (Balearic Islands, Spain; Western Mediterranean), using a 2-fold approach, allowed the recognition of anomalies consistent with traumatic fractures, infections, neoplasms, and probable congenital malformations. These pathological remains constitute the first documented evidence of disease in certain endemic vertebrate species and genera, with some cases being particularly unusual and rare, previously undiagnosed in either extinct or extant relatives. The occurrence of disorders in extinct insular species is not uncommon and can be attributed to the particular selective pressures of islands (including low extrinsic mortality rates and resource limitation) and their life history eco-evolutionary responses. The findings of our study expand the biological knowledge of these 3 extinct taxa from an interdisciplinary perspective, while also contributing to a broader understanding of vertebrate zoology under insular regimes through empirical observations.

Studies focusing on the prevalence and incidence of pathological conditions in wildlife populations are essential for achieving a deeper biological and ecological interpretation of abnormal fossil findings and for shedding light on this phenomenon. The distinctive morphological convergences observed in extinct insular mammals (such as dwarfism and gigantism) have historically sparked interest within the scientific community (Sondaar 1977; Palombo and Moncunill-Sol 2025), with islands being viewed as repeatable and testable natural laboratories for exploring biogeographical, ecological, and evolutionary processes and patterns. Although paleopathological disorders reported in extinct insular species to date have often been considered mere curiosities or of taxonomical interest, quantitative studies' prevalence assessments can significantly contribute to a broader understanding of the evolutionary processes that shaped vertebrates under insular regimes, including their generalities, mechanisms, and drivers.

Acknowledgments

The authors would like to acknowledge the use of "Sección de Tomografía, Área de Infraestructuras de Investigación, Universidade de Santiago de Compostela," with special thanks to Dr. M. Candás Romero (Estación de Bioloxía Mariña da Graña) for her assistance in the preparation of CT scans. The authors would also like to thank Dr. J.M. Robles for providing access to the study material housed in the ICP collections.

Authors' contributions

Conceptualization: B.M.-S., J.Q.C.; formal analysis: B.M.-S., A.B., B.M.R.; investigation: B.M.-S.; resources: B.M.-S., J.Q.C., A.B.; data curation: B.M.-S., A.B.; writing—original draft: B.M.-S., B.M.R.; writing—review & editing: J.Q.C., A.B., B.M.R.; visualization: B.M.-S., A.B.; funding acquisition: B.M.-S., J.Q.C.

Funding

Xunta de Galicia supports this work through project ED431B 2024/03 and ED431F 2023/36 from the programme "Axudas para a consolidación e estructuración de unidades de investigación competitivas e outras acción de fomento nas universidades do Sistema universitario de Galicia (SUG)". B.M.-S. is supported by ED481D-2022-013 (funded by Consellería de Cultura, Educación e Universidades, Xunta de Galicia) and 101180634 – REvoBBIT (ERA Fellowship, HORIZON-TMA-MSCA-PF-EF), funded by European Union. Views and opinions expressed are those of the author(s) only and do not necessarily reflect those of the EU, who cannot be held responsible for them. J.Q.C. receives funding of the R+D+I project PID2020-117118GB-I00/AEI/10.13039/501100011033, funded by the Agencia Estatal de Investigación of the Spanish Ministerio de Ciencia e Innovación, and his research is also supported by the Generalitat de Catalunya/CERCA Programme. A.B. is funded by the "Ramón y Cajal" fellowship RYC2021-034269-I, funded by MCIN/AEI/10.13039/501100011033 and the European Union «NextGenerationEU»/PRTR. Funding for open access charge: Universidade da Coruña/CISUG.

Conflicts of interest

The authors declare that they have no conflict of interest.

Ethics statement

The research involved only the analysis of fossil material. No live animals were involved and no animal experiments were performed. All assessed specimens were collected and housed in the open scientific collections in accordance with relevant legal and institutional guidelines.

Artificial intelligence (AI)-assisted technologies

The authors declare that AI-assisted technologies were not used to design experiment, generate scientific content and data, analyze results, or interpret findings. All scientific conclusions and interpretations are the sole work of the authors.

Supplementary material

Supplementary material can be found at https://academic.oup.com/cz.

Downloaded from academic.oup.com/cz/advance-article/doi/10.1093/cz/zoag023/8556684 by guest on 23 October 2026

Data availability

All data necessary to support the conclusions of this study are provided within the article and its supplementary materials. The analyzed fossil specimens are housed in institutional collections and are available for study upon reasonable request. The volumetric image series of the specimens are hosted on the online 3D scientific data repository MorphoSource (https://www.morphosource.org/projects/000758818). Additional information is available from the corresponding author upon reasonable request.

References

Albuquerque TAF, Drummond do Val L, Doherty A, de Magalhães JP, 2018. From humans to hydra: patterns of cancer across the tree of life. *Biol Rev Camb Philos Soc* **93**(3):1715–1734.

Alcover JA, Moyà-Solà S, Pons-Moyà J, 1981. *Les quimeres del passat: els vertebrats fòssils del Plio-Quaternari de les Balears i Pitiüses*. Ciutat de Mallorca: Editorial Moll. [Catalan]

Andrews CW, 1915. A description of the skull and skeleton of a peculiarly modified rupicaprine antelope (*Myotragus balearicus*), with a notice of a new variety, *M. balearicus* var. *major*. *Philos Trans R Soc Lond B* **206**(325–334):281–305.

Appleby J, 2022. Differential diagnosis and rigor in paleopathology. In: Grauer AL, editor. *The Routledge Handbook of Paleopathology*. London: Routledge Taylor & Francis Group, 43–63.

Baker J, Brothwell D, 1980. *Animal Diseases in Archaeology*. London: Academic Press.

Biton R, Geffen E, Vences M, Cohen O, Bailon S *et al.*, 2013. The rediscovered Hula painted frog is a living fossil. *Nat Commun* **4**(1):1959.

Bodinga HA, Nura A, Bande F, Abubakar AA, Yakubu AS *et al.*, 2020. Congenital malformations in ruminants and its surgical management: a retrospective study of Sokoto veterinary clinic, Nigeria. *Int J Sci Rep* **6**(7):248–252.

Bover P, Alcover JA, 1999. The evolution and ontogeny of the dentition of *Myotragus balearicus* Bate, 1909 (Artiodactyla, Caprinae): evidence from new fossil data. *Biol J Linn Soc* **68**(3):401–428.

Bover P, Llamas B, Mitchell KJ, Thomson VA, Alcover JA *et al.*, 2019. Unraveling the phylogenetic relationships of the extinct bovid *Myotragus balearicus* Bate 1909 from the Balearic Islands. *Quat Sci Rev* **215**:185–195.

Brothwell D, Sandison AT, 1967. Editorial prolegomenon: the present and future. In: Brothwell D, Sandison AT, editors. *Disease in Antiquity: A Survey of the Diseases, Injuries and Surgery of Early Populations*. Springfield: Charles C. Thomas, xi–xiv.

Brown C, Rinaldi CE, Ripple WJ, Van Valkenburgh B, 2020. Skeletal and dental development preserve evidence of energetic stress in the moose of Isle Royale. *Front Ecol Evol* **8**:272.

Cagan A, Baez-Ortega A, Brzozowska N, Abascal F, Coorens THH *et al.*, 2022. Somatic mutation rates scale with lifespan across mammals. *Nature* **604**(7906):517–524.

Canpolat I, Karabulut E, Cakir S, 2017. The effect on production loss of dental disorders in adult goats. *IOSR J Agric Vet Sci* **10**:76–80.

Capello V, 2004. Diagnosis and treatment of dental disease in pet rabbits and rodents: a review. *Exot Mammal Med Surg* **2**(2):5–12.

Christie ALM, Lee MXY, Evenhuis JV, Rickert SS, Kass PH *et al.*, 2023. Dental and temporomandibular joint pathology of the island fox (*Urocyon littoralis*). *J Comp Pathol* **200**:23–34.

Compton ZT, Mellon W, Harris VK, Rupp S, Mallo D *et al.*, 2025. Cancer prevalence across vertebrates. *Cancer Discov* **15**(1):227–244.

Corbera JA, Morales I, Martín S, Arencibia A, Gutierrez C, 2017. A case of congenital supernumerary teeth in an ovine dental pad. *J Vet Dent* **34**(4):279–281.

Densmore C, Green DE, 2007. Diseases of amphibians. *ILAR J* **48**(3):235–254.

Dermitzakis M, van der Geer AAE, Lyras G, 2006. Paleopathological observations on a population of fossil deer from the Late Pleistocene of Crete. In: Kalofourtis A, Papadopoulos N, Spiliopoulou C *et al.* editors. *Volume in Honor of Professor Andonis Koutselinis*. Athens: Parisianou Editions, 43–51.

Esper JF, 1774. *Ausführliche Nachricht von neuentdeckten Zoolithen unbekannter vierfüsiger Thiere, und denen sie enthaltenden, so wie verschiedenen andern denkwürdigen Grüften der Obergebürgischen Lande des Marggrafthums Bayreuth*. Nürnberg: Georg Wolfgang Knorr. [German]

Faria JF, Megía-Palma R, Harris DJ, 2024. Impact of blood parasites on the behaviour of two congenital wall lizards (genus *Podarcis*). *Behav Ecol Sociobiol* **78**(10):105.

Fernández-Bejarano E, Blanco A, Angelone C, Zhang Z, Moncunill-Solé B, 2024. Bone histology of the Late Pleistocene *Prolagus sardus* (Lagomorpha: Mammalia) provides further insights into life-history strategy of insular giant small mammals. *Zool J Linn Soc* **201**(1):169–183.

Gazendam A, Popovic S, Parasu N, Ghert M, 2023. Chondrosarcoma: a clinical review. *J Clin Med* **12**(7):2506.

Grauer AL, 2012. Introduction: the scope of paleopathology. In: Grauer AL, editor. *A Companion to Paleopathology. Blackwell Companions to Anthropology*. West Sussex: Blackwell Publishing Ltd, 1–14.

Grauer AL, 2022. *The Routledge Handboook of Paleopathology*. London: Routledge Taylor & Francis Group.

Gray HM, Ouellet M, Green DM, 2002. Traumatic injuries in two neotropical frogs, *Dendrobates auratus* and *Physalaemus pustulosus*. *J Herpetol* **36**(1):117–121.

Green DE, Harshbarger JC, 2001. Spontaneous neoplasia in amphibia. In: Wright KM, Whitaker BR, editors. *Amphibian Medicine and Captive Husbandry*. Malabar: Krieger Publishing Company, 335–400.

Ippen R, Heinrich W-D, 1977. Pathologische Veränderungen an fossile Extremitäten-Knochen von Anuren aus dem fossilen Tierbautensystem von Pisede bei Malchin. *Wiss Z Humboldt-Univ Berlin* **26**:301–305. [German]

Jordana X, Galtés I, Isidro A, Malgosa A, Köhler M *et al.*, 2011. Estudio macroscópico, radiológico y histológico de una fractura tibial de *Myotragus balearicus*. In: González Martín A, Cambra-Moo O, Rascón Pérez J, editors. *Paleopatología: Ciencia Multidisciplinar*. Madrid: Universidad Autónoma de Madrid, 435–439. [Spanish]

Downloaded from academic.oup.com/cz/advance-article/doi/10.1093/cz/zoag023/8556684 by guest on 23 October 2026

Knafo SE, 2019. Musculoskeletal system. In: Divers SJ, Stahl SJ, editors. *Mader's Reptile and Amphibian. Medicine and Surgery*. 3rd edn. Missouri: Elsevier, 894–916.

Lyras GA, Giannakopoulou A, Lillis T, van der Geer AAE, 2019. Paradise lost: evidence for a devastating metabolic bone disease in an insular Pleistocene deer. *Int J Paleopathol* **24**: 213–226.

Lyras GA, Giannakopoulou A, Lillis T, Veis A, Papadopoulos GC, 2016. Bone lesions in a Late Pleistocene assemblage of the insular deer *Candiacervus* sp.II from Liko cave (Crete, Greece). *Int J Paleopathol* **14**:36–45.

Maempel GZ, 1993. Skeletal pathology and congenital variations in the Maltese pleistocene hippopotamus. *J Zool* **231**(1): 157–162.

Meuten DJ, 2017. *Tumors in Domestic Animals*. 5th edn. Iowa: Wiley Blackwell.

Micheletti Cremasco M, Merlo F, Fulcheri E, Rothschild BM, 2015. Tropical ulcer on a human tibia from 5000 years ago in Northern Italy. *Int J Osteoarchaeol* **25**(5):788–794.

Moncunill-Solé B, 2021. Eco-evolutionary adaptations of ochotonids (Mammalia: Lagomorpha) to islands: new insights into Late Miocene pikas from the Gargano palaeo-archipelago (Italy). *Biol J Linn Soc* **132**(2):400–413.

Moncunill-Solé B, Arzi B, Filliquist B, Vapniarsky N, Zavodovskaya R *et al.*, 2024. The extinct osteoarthritic lagomorphs (*Prolagus sardus*) from Sardinia (Italy) reveal further evidence of life history evolution in insular domains. *Palaeoworld* **33**(2):504–516.

Moncunill-Solé B, Isidro A, Blanco A, Angelone C, Rössner GE *et al.*, 2019. The most ancient evidence of a diseased lagomorph: infectious paleopathology in a tibiofibular bone (Middle Miocene, Germany). *C R Palevol* **18**(8):1011–1023.

Moodie RL, 1927. Tumors in the lower Carboniferous. *Science* **66**(1718):540.

Olmacher HP, 1898. Several examples illustrating the comparative pathology of tumours. *Bull Ohio Hosp Epileptics* **1**: 223–236.

Palkovacs EP, 2003. Explaining adaptive shifts in body size on islands: a life history approach. *Oikos* **103**(1):37–44.

Palombo MR, Moncunill-Solé B, 2025. Dwarfing and gigantism in Quaternary vertebrates. In: Elias S, editor. *Encyclopedia of Quaternary Science*, **Vol. 6**. 3rd edn. Amsterdam: Elsevier BV, 584–608.

Palombo MR, Zedda M, 2016. Surviving in a predator-free environment: hints from a bone remodeling process in a dwarf Pleistocene deer from Crete. *C R Palevol* **15**(1–2):245–254.

Palombo MR, Zedda M, 2022. The intriguing giant deer from the Bate cave (Crete): could paleohistological evidence question its taxonomy and nomenclature? *Integr Zool* **17**(1):54–77.

Perl RGB, Gafny S, Malka Y, Renan S, Woodhams DC *et al.*, 2017. Natural history and conservation of the rediscovered Hula painted frog, *Latonia nigriventer*. *Contrib Zool* **86**(1):11–37.

Peterson RO, Vucetich JA, Fenton G, Drummer TD, Larsen CS, 2010. Ecology of arthritis. *Ecol Lett* **13**(9):1124–1128.

Pritchard JJ, Ruzicka AJ, 1950. Comparison of fracture repair in the frog, lizard and rat. *J Anat* **84**:236–261.

Resnick D, 2002. *Diagnosis of Bone and Joint Disorders*. Philadelphia: WB Saunders Company.

Resnick D, Kyriakos M, Greenway GD, 2002. Tumors and tumor-like lesions of bone: imaging and pathology of specific lesions. In: Resnick D, editor. *Diagnosis of Bone and Joint Disorders*. 4th edn. Philadelphia: WB Saunders Company, 3800–3833.

Rothschild B, 2009. Scientifically rigorous reptile and amphibian osseous pathology: lessons for forensic herpetology from comparative and paleo-pathology. *Appl Herpetol* **6**(1):47–79.

Rothschild B, 2010. Macroscopic recognition of nontraumatic osseous pathology in the postcranial skeletons of crocodilians and lizards. *J Herpetol* **44**(1):13–20.

Rothschild BM, Laub RS, 2013. Epidemiology of anuran pathology in the Holocene component of the Hiscock site: rare or not survived. *J Herpetol* **47**(1):169–173.

Rothschild B, Martin L, 2006. Skeletal impact of disease. *New Mex Mus Nat Hist Sci Bull* **33**:1–12.

Rothschild B, Naples V, Barbian L, 2006. Bone manifestations of actinomycosis. *Ann Diagn Pathol* **10**(1):24–27.

Rothschild B, Robinson L, Witt M, Koay J, Cline H, 2018. Radiologic/histologic discrepancies in tumour identification: the case of a "basketball-sized" mandibular tumour in a woman from 17th century West Virginia. *Int J Osteoarchaeol* **28**(6): 775–781.

Rothschild B, Schultze HP, Pellegrini R, 2013. *Herpetological Osteopathology. Annotated Bibliography of Amphibians and Reptiles*. New York: Springer.

Rothschild BM, Surmik D, Bertozzo F, 2023. *Modern Paleopathology. The Study of Diagnostic Approach to Ancient Diseases, Their Pathology and Epidemiology. Let There be Light, the Light of Science and Critical Thinking*. Cham: Springer Nature Switzerland AG.

Sanchiz FB, Pérez JP, 1974. Frecuencia de anomalías óseas en la población de *Discoglossus pictus* (Anura, Discoglossidae) de Campos (Asturias). *Bol Estac Cent Ecol* **6**:69–77. [Spanish]

Schlumberger HG, Lucke B, 1948. Tumors of fishes, amphibians, and reptiles. *Cancer Res* **8**:657–753.

Shannon JG, Woolhouse FM, Eisinger PJ, 1973. The treatment of chronic osteomyelitis by saucerization and immediate skin grafting. *Clin Orthop Relat Res* **96**(1):98–107.

Skutschas P, Kolchanov V, Boitsova E, Kuzmin I, 2018. Osseous anomalies of the cryptobranchid *Eoscapherpeton asiaticum* (Amphibia: Caudata) from the Late Cretaceous of Uzbekistan. *Foss Rec* **21**(1):159–169.

Sondaar PY, 1977. Insularity and its effect on mammal evolution. In: Hecht MK, Goody PC, Hecht BM, editors. *Major Patterns in Vertebrate Evolution*. New York: Plenum Publishing Corporation, 671–707.

Sorbelli L, Azzarà B, Cherin M, Delfino M, Roček Z *et al.*, 2025. Why extant, why not extinct? A new extinct *Latonia* species (Anura: Discoglossidae) from the Early Pleistocene of the Apennine Peninsula provides clues on the survival of the genus in Eurasia. *J Syst Palaeontol* **23**(1):2554727.

Speybroeck J, Beukema W, Dufresnes C, Fritz U, Jablonski D *et al.*, 2020. Species list of the European herpeto-fauna—2020 update by the Taxonomic Committee of the Societas Europaea Herpetologica. *Amphib Reptil* **41**(2):139–189.

Špinar Z, 1972. *Tertiary Frogs from Central Europe*. Prague: Academia.

Storniolo F, Zuffi MAL, Coladonato AJ, Mangiacotti M, Scali S *et al.*, 2022. Haemospodridian infections in wild populations of *Podarcis muralis* from the Italian Peninsula. *Parasitology* **149**(9):1179–1185.

Downloaded from academic.oup.com/cz/advance-article/doi/10.1093/cz/zoag023/8556684 by guest on 23 October 2026

Thompson KG, Dittmer KE, 2017. Tumors of bone. In: Meuten DJ, editor. *Tumors in Domestic Animals*. 5th edn. Iowa: Wiley Blackwell, 356–424.

Vasconcelos J, dos Anjos Pires M, Alves A, Vieira-Pinto M, Saraiva C *et al.*, 2023. Neoplasms in domestic ruminants and swine: a systematic literature review. *Vet Sci* **10**(2):163.

Verstraete FJM, van Aarde RJ, Nieuwoudt BA, Mauer E, Kass PH, 1996. The dental pathology of feral cats on Marion Island, part II: periodontitis, external odontoclastic resorption lesions and mandibular thickening. *J Comp Pathol* **115**(3): 283–297.

Villa A, Delfino M, 2019. Fossil lizards and worm lizards (Reptilia, Squamata) from the Neogene and Quaternary of Europe: an overview. *Swiss J Palaeontol* **138**(2):177–211.

Waldren W, Kopper JS, 1968. *Myotragus balearicus. Paleopathology and palynological analysis of the soil of the deposit*. Vol. **5**. Mallorca: Deya Archaeological Museum.

Waldron T, 2009. *Paleopathology*. New York: Cambridge University Press.

Waldron T, 2012. Joint disease. In: Grauer AL, editor. *A Companion to Paleopathology. Blackwell Companions to Anthropology*. West Sussex: Blackwell Publishing, 513–530.

White EI, 1927. The fish-fauna of the cementstones of Foulden, Berwickshire. *Trans Roy Soc Edinburgh* **55**(1):255–287.

Whitney MR, Mose L, Sidor CA, 2017. Odontoma in a 255-million-year-old mammalian forebear. *JAMA Oncol* **3**(7): 998–1000.

Whittaker RJ, Fernández-Palacios JM, 2007. *Island Biogeography: Ecology, Evolution, and Conservation*. 2nd edn. Oxford: Oxford University Press.

Wilson DW, 2017. Tumors of the respiratory tract. In: Meuten DJ, editor. *Tumors in Domestic Animals*. 5th edn. Iowa: Wiley Blackwell, 467–498.

Witzmann F, Asbach O, 2022. Disease in the fossil record. In: Grauer AL, editor. *The Routledge Handboook of Paleopathology*. London: Routledge Taylor & Francis Group, 541–556.

Witzmann F, Haridy Y, Hilger A, Manke I, Asbach P, 2021. Rarity of congenital malformation and deformity in the fossil record of vertebrates—A non-human perspective. *Int J Paleopathol* **33**: 30–42.

Wolff EDS, 2007. *Oral Pathology of the Archosauria. Bony Abnormalities and Phylogenetic Inference*. D. Phil. Thesis. Montana State University.

Wood JW, Milner GR, Harpending HC, Weiss KM, 1992. The osteological paradox. Problems of inferring prehistoric health from skeletal samples. *Curr Anthropol* **33**(4):343–370.

Wu S, Pan Y, Mao Y, Chen Y, He Y, 2021. Current progress and mechanisms of bone metastasis in lung cancer: a narrative review. *Transl Lung Cancer Res* **10**(1):439–451.

Zoboli D, Zedda M, Pillola GL, Palombo MR, 2018. Does a relationship exist between palaeopathologies and insularity? A case study of some bone of *Prolagus sardus* (Wagner, 1829) from Sardinia (Italy). *Alp Mediterr Quat* **31**:75–86.

Downloaded from academic.oup.com/cz/advance-article/doi/10.1093/cz/zoag023/8556684 by guest on 23 October 2026